UNIVERSIDADE FEDERAL DE SANTA CATARINA

JÚLIA KINA COLELLA FERRO

INDIGO CARMINE REMOVED USING GEOPOLYMERS FROM RICE HUSK ASH AS ADSORBENT

Araranguá, SC
2018

JÚLIA KINA COLELLA FERRO

INDIGO CARMINE REMOVED USING GEOPOLYMERS FROM RICE HUSK ASH AS ADSORBENT

Trabalho de Conclusão de Curso, apresentado à Universidade Federal de Santa Catarina, como parte das exigências para a obtenção do título de Engenheiro(a) de Energia.

Araranguá, 26 de junho de 2018.

BANCA EXAMINADORA

Tatiana Pineda V.

Profa. Dra. Tatiana Gisset Pineda Vásquez (Orientadora)
Universidade Federal de Santa Catarina

Elise Sommer Watzko

Profa. Dra. Elise Sommer Watzko
Universidade Federal de Santa Catarina

Profa. Dra. Regina Vasconcellos Antonio
Universidade Federal de Santa Catarina

ABSTRACT

Batch adsorption removal of Indigo Carmine (IC) from aqueous solution onto a new type of geopolymer synthesized from two industrial wastes rice husk ash (RHA) and ceramic residues (CR) was investigated under different conditions. It was found that the most favorable condition for adsorbent dose was 0.04 g/mL in the concentration of 50 mg/L and a contact time of 120 minutes. The percentage removal at initial concentrations of IC for 50 mg/L was approximately 99%. The kinetic studies showed that adsorption process follows the pseudo second-order. The effect of temperature on the adsorption capacity and the percentage removal of IC was also studied. Finally, the equilibrium adsorption data were well represented by Freundlich and Temkin adsorption models. The maximum adsorption capacity for IC was 1.35 mg/g at 323 K with an initial concentration of 65 mg/L. Therefore this geopolymer can be used as adsorbent for the removal of Indigo Carmine from textile industry wastewater.

Keywords: Indigo Carmine, Geopolymer, Rice Husk Ash, Adsorption.

1 INTRODUCTION

Wastewater from textile industries frequently contains significant amounts of non-biodegradable dyes (PALMA-GOYES et al., 2014). Most of the dyes are toxic and carcinogenic, hereby posing serious threats to living organisms (SOOD et al., 2015). Of all the dyes produced in the world, 11% is lost in effluents during manufacture and application processes (RAUF; ASHRAF, 2009). Indigo Carmine (IC) is a blue dye, considered a highly toxic indigoid class of dye and constitutes one of the most important groups of pollutants found in wastewater from textile industries (LABIADH et al., 2017). For these reasons, is very important to efficiently treat the effluents before being discharged.

The optimization of wastewater purification processes requires a development of new operations based on low cost raw materials with high pollutant-removal efficiency (PERIĆ; TRGO; VUKOJEVIĆ MEDVIDOVIĆ, 2004). For that reason, geopolymers appear as a recent technology, since it has shown from many researches good adsorption properties (ARIFFIN et al., 2017). Besides it has been proven that geopolymers have a low cost, especially if its composition is based on residues already available and the low energy requirements of production (BAKHAREV, 2006). Geopolymers are inorganic polymers resulted from the polymerization process and in order for this to happen is necessary the use of raw-materials rich in alumina and silica and a high alkaline solution as the activator source (DAVIDOVITS, 1982).

Since geopolymers need a source for silica and alumina, the rice husk ash (RHA) and the ceramic residue (CR) can be great materials for this application. RHA is basically composed by silica (70%) and CR is composed essentially by alumina (58%) and silica (11%) (COLELLA et al, 2017). Other studies have shown that the low-cost geopolymer can be used as an adsorbent for Indigo Carmine (IC) removal from aqueous solutions (LAKSHMI et al., 2009).

The present study proposes to use geopolymers based on rice husk ash and ceramic industry waste as an adsorbent for the removal of IC from aqueous solutions and to contribute with a new technology with a low cost adsorbent for adsorption processes from industrial wastewater, thus to encourage future research and further works in the area.

2 LITERATURE REVIEW

In this section, the literature review will be presented, which covers the recent studies around the subject. Furthermore, it is also defined some basic concepts for a better understanding of the subject.

2.1 Indigo Carmine

Indigo Carmine dye (IC) is mainly used in the dyeing of clothes (blue jeans), as indicator in analytical chemistry and as a microscopic stain in biology (AMMAR et al., 2006). IC is considered as high toxic indigoid class of dye. Contact with it causes skin and eye irritations, it also cause permanent injury to cornea and conjunctiva (OTHMAN; MOHAMED; IBRAHEM, 2007). The consumption of the dye was also proven to be fatal, as it is carcinogenic and can lead to reproductive, developmental, neuron and acute toxicity (NACIRI et al., 2016).

The wasted dyes released in the effluent interfere with the transmission of light in the water bodies that receive this effluent. This in turn inhibits the photosynthetic activity of aquatic biota besides direct toxic effects on biota (LAKSHMI et al., 2009). In addition, these dyes can be accumulated in aquatic animals and, consequently, get into the alimentary chain and reach human beings (ARENAS et al., 2017). Figure 1 illustrates the chemical structure of Indigo Carmine.

Figure 1 – Chemical Structure of Indigo Carmine.

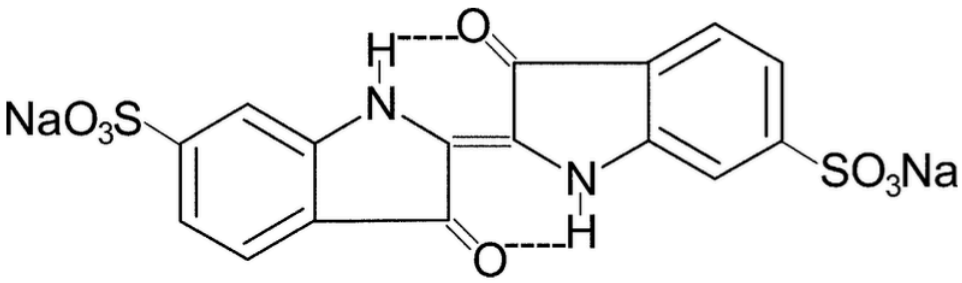

Source: (MITTAL; MITTAL; KURUP, 2006)

2.2 Geopolymer

Geopolymer is a new class of inorganic polymer synthesized by activation of an aluminosilicate source with an alkaline hydroxide or silicate solution at ambient temperature,

which was first developed by Davidovits in the late 1970s (DAVIDOVITS, 1991; HUANG; HAN, 2011).

The synthesis of geopolymer is normally carried out by mixing aluminosilicate reactive materials with strong alkaline solutions, usually sodium hydroxide, then curing the mixture at temperatures between 20 and 100 ˚C. Such under conditions, aluminum and oxygen atoms create a chain of SiO_4 and AlO_4 tetrahedral linked alternatively by shared oxygen atoms (MAJIDI, 2009). These units are then gradually split out with the development of the reaction, and linked alternatively to yield polymeric precursors by sharing all oxygen atoms between two tetrahedral units, and thereby forming monolithic like geopolymer products (AL-ZBOON; AL-HARAHSHEH; HANI, 2011). A schematic diagram of typical geochemical reactions associated with mineral polymer and geopolymer formation is provided in Figure 2 (LI; WANG; ZHU, 2006).

Figure 2 – Schematic of the reaction pathway for geopolymerization.

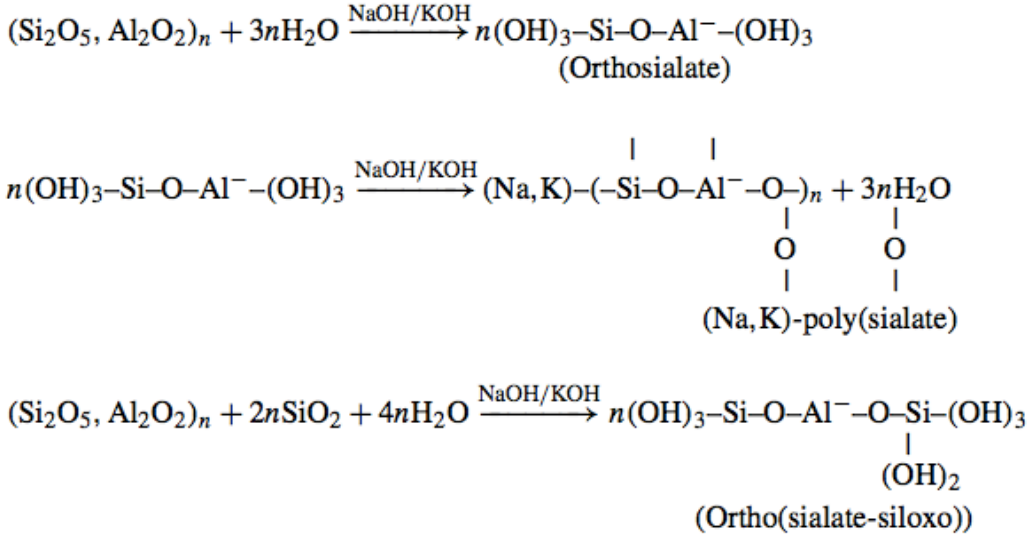

Source: (LI; WANG; ZHU, 2006)

Figure 3 – Schematic diagram of geopolymer formation

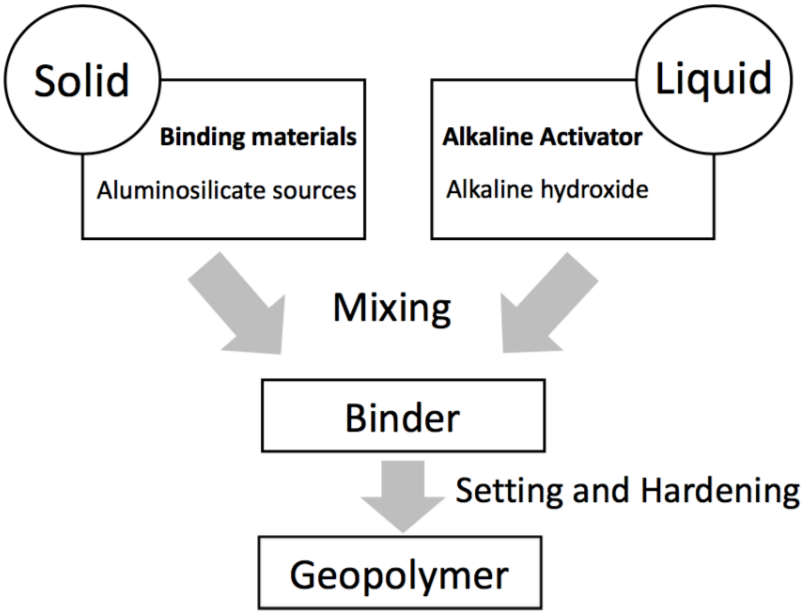

Source: Adapted from (LIEW et al., 2016).

Geopolymers can be used as an additive for manufacturing process of Portland cement, providing a more environmentally friendly alternative. The use of geopolymers can reduce up to 90% on the CO_2 emissions compared to Portland cement (DAVIDOVITS, 2013). Also, it can be used for adsorption of heavy metals from aqueous solutions. In addition, a recent study presented that geopolymers can be used as a coating to protect reinforced concrete against corrosion, with excellent geopolymer characteristics, such as mechanical strength, chloride permeability and electrical resistivity (AGUIRRE-GUERRERO; ROBAYO-SALAZAR; DE GUTIÉRREZ, 2017).

Alternative low-cost, non-conventional adsorbents such as bagasse fly ash, rice husk ash, peat, lignite, bagasse pith, wood, saw dust, etc. have been investigated for the treatment of effluents (SRIVASTAVA; MALL; MISHRA, 2007). Besides, depending on the raw material selection and processing conditions, geopolymers can exhibit a wide variety of properties and characteristics, including high compressive strength, low shrinkage, fast or slow setting, acid resistance, fire resistance and low thermal conductivity (DUXON et al., 2007). Many researches have shown a high adsorption capacity with geopolymers based on low cost materials, such as ash, agricultural and solid waste (AL-HARAHSHEH et al., 2015; ARIFFIN et al., 2017).

2.3 Rice Husk Ash

Rice is a staple food of over half the world's people (MARASENI et al., 2018). This includes Brazil, which is the eighth largest rice producer in the world (FAO, 2017), in total 10.5 million tonnes of rice were produced in the 2015/2016 harvest (CONAB, 2016). For this reason, there are a large quantity of byproducts produced in this industry. One of them is the rice husk, obtained from the rice mills after the separation of rice from paddy. In nature, rice husk is tough, insoluble in water, woody and characterized by its abrasive inherent resistance behavior and silica-cellulose structural arrangement (DAIFULLAH; GIRGIS; GAD, 2003).

Traditionally, rice husks have been disposed in landfills, but environmental regulations have limited this, resulting in a need for increased utilization (KAMATH; PROCTOR, 1998). Because of that and the arising preoccupation about more environment-friendly industries, people are trying to reuse the rice husk. For that matter, its principal application is as an ideal source for power plants in the rice mill industry, since it has a higher heating value (QUISPE; NAVIA; KAHHAT, 2017).

Rice husk ash (RHA) is collected from the particulate collection equipment attached upstream to the stack of the rice husk-fired boilers (LAKSHMI et al., 2009). It is estimated that the generation rate is approximately 0.046 tonne for every tonne of rice produced (FOO; HAMEED, 2009). RHA is composed by approximately 70% of silica (SiO_2) and some metals in the oxide form in less quantity (COLELLA et al, 2017). The nature of the silica in RHA is mainly amorphous which means a structure formed by atoms with short-distance orientation, making it highly reactive (ARENAS et al., 2017).

RHA has been used for removal of different pollutants from aqueous solution such as brilliant green dye (TAVLIEVA et al., 2013), IC (ARENAS et al., 2017) and toxic metal ions (FENG et al., 2004; SRIVASTAVA; MALL; MISHRA, 2007). One of the parameters that is important for the adsorption process is the particle size of the RHA. For that reason, some of the researches have reported the particle size for the RHA as an adsorbent. Kumar et al (2008) concluded that for the lead ion adsorption the particle size used was between 250 and 350 μm and the adsorption process efficiency using industrial effluents was found to be 96.83% (KUMAR et al., 2009). Another study showed a high removal of the dyes Methylene Blue and Congo Red from aqueous solution with a particle size of the RHA of 212 μm (CHOWDHURY;

SARKAR; BANDYOPADHYAY, 2009). In addition, another research presented a 150 μm RHA particle size (TORKAMAN; ASHORI; MOMTAZI, 2013).

2.4 Ceramic Waste

In the ceramic process, approximately 30% of the materials become residues and currently are not reused in any way (AWOYERA et al., 2016). Nowadays, these residues are deposited directly in landfills (ZIMBILI; SALIM; NDAMBUKI, 2014). This way, recycle can be an alternative to reduce the extraction demand and landfill pressures, conducting to a better sustainability of the resources (SILVESTRE et al., 2013). Besides all that, according to National Cement Association (ANFACER), Brazil is the second largest producer of ceramics in the world, consequently it is necessary to have ways to reuse this residue.

The traditional and most used ceramic process starts with the mixture and homogenization of the raw materials. After that the material is milled, so the atomization can take place. In the atomization, a paste is formed so it is possible to shape it and then dry it. After the drying process, it is glazed and finally it is submitted to a fast firing. A schematic diagram of the ceramic process is shown in Figure 4.

Figure 4 – Traditional ceramic process production.

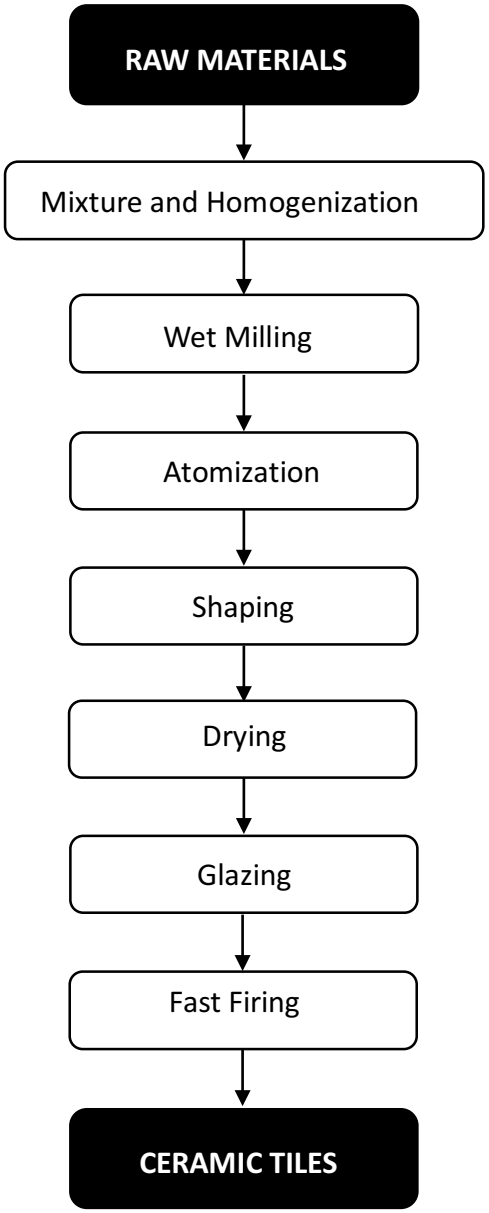

Source: Adapted from (CASASOLA; RINCÓN; ROMERO, 2012)

2.5 Water treatment through adsorption

There are many methods that have been developed for the removal of synthetic dyes waters and wastewaters to decrease their impact on the environment (OROS; FORGACS; CSERHATI, 2004). These techniques can be divided in three categories: chemical, physical or biological process. The chemical process includes electrochemical oxidation (AMMAR et al., 2006; PALMA-GOYES et al., 2014), coagulation, flocculation (LIANG et al., 2014) and photocatalytic degradation (SOOD et al., 2015). Although these processes can be economically

feasible, it has a high sludge formation decreasing its effectiveness (AHMED; AHMARUZZAMAN, 2016).

The biological treatment consists in the dye degradation by metabolic pathways or adsorption with biomass (PAZ et al., 2017). However when using enzymes the production shown to be unreliable and not effective for all dyes (YAGUB et al., 2014). The physical process includes membrane filtration, ion exchange and adsorption. Among to all these methods, physical treatments such as adsorption are recognized as a well stablished technique to remove toxic compounds from water and wastewater (ARENAS et al., 2017).

Adsorption is a surface phenomenon that is defined as the increase in concentration of a particular component at the surface or interface between two phases (FAUST; ALY, 1983). Figure 5 illustrates the basic concepts for adsorption process.

Figure 5 – Basic terms for adsorption and its principle.

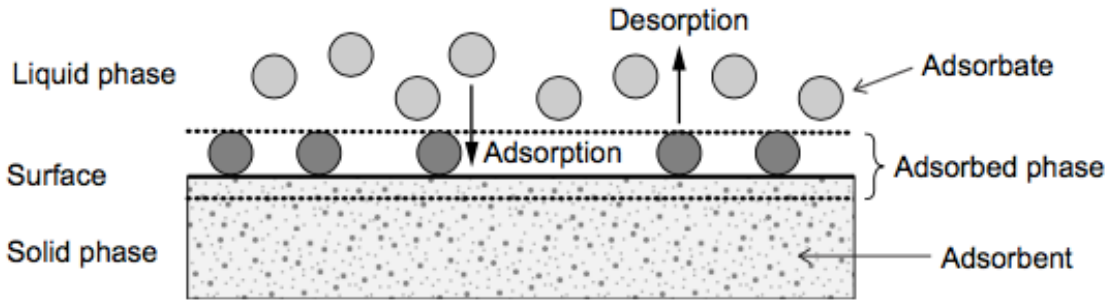

Source: (WORCH, 2012)

The solid phase provides the site for adsorption and is considered the adsorbent; while the the liquid phase will be adsorbed, is referred to as the adsorbate. In some cases, the adsorption process can be reversed and the adsorbate returns to the liquid phase, being referred to as desorption.

This process can be affected by different parameters such as, temperature, the nature of the adsorbate and adsorbent, the presence of other compounds and experimental conditions (like pH, concentration of pollutant, contact time and particle size of the adsorbent) (ALI; GUPTA, 2007).

The adsorption for waste and wastewater treatment works over different materials that have been proved for removing IC from wastewater effluents such as activated carbon (HU et al., 2016), biomaterials such as chitin and chitosan (PRADO et al., 2004) and fly ash (CARVALHO et al., 2011) with promising results.

2.5.1 Adsorption kinetics

The adsorption kinetics was studied because it permits elucidation of adsorption mechanisms in the treatment of dye containing industrial effluents. Its study enables to examine and to understand the controlling mechanisms of adsorption process and helps determine the process efficiency (ARENAS et al., 2017). There are various models for the different combination of adsorbate and adsorbent, where the adsorption process has been considered as being of a pseudo-first order, a pseudo-second order, controlled by intra-particle diffusion, chemisorption and many others (GEORGIEVA et al., 2015).

The pseudo-first order kinetic model was suggested by Lagergren (LAGERGREN, 1898) for the adsorption of solid/liquid systems and its formula is given as described in Equation 1.

$$\log(q_e - q_t) = log\ q_e - k_{PFO}t \tag{1}$$

where q_e and q_t (mg/g) are the amounts of adsorbate adsorbed at equilibrium and at any time t (min), respectively and k_{PFO} is the adsorption rate constant. From the plot of $\log(q_e - q_t)$ versus t it is possible to determine the slope (k_{PFO}) and intercept ($log\ q_e$) (TAN; AHMAD; HAMEED, 2009).

Many researchers demonstrated that the adsorption process is better describe with the pseudo-second order model (CHOWDHURY; SARKAR; BANDYOPADHYAY, 2009; LAKSHMI et al., 2009; TAVLIEVA et al., 2013). This model takes into consideration that adsorption reaction onto the surface of adsorbent is the rate controlling step and has been most widely used to describe time evolution of adsorption under non-equilibrium conditions. Pseudo-second order model is described by Equation 2, where q_e and q_t are respectively the amounts of adsorbate at equilibrium and at any time (t); and k_{PSM} is the pseudo-second order rate constant [g/(mg min)] (ARENAS et al., 2017; HO; MCKAY, 1999).

$$q_t = \frac{t\ k_{PSO}\ q_e^2}{1 + t\ k_{PSO}\ q_e} \tag{2}$$

The linear form of Equation 3 can be represented as follows:

$$\frac{t}{q_t} = \frac{1}{k_{PSO} q_e^2} + \frac{1}{q_e} t \tag{3}$$

According to Equation 3, plotting t/q_t versus time t gives a straight line which the slope is $1/(k_{PSO}q_e^2)$ and the intercept is $1/q_e$ (SENTHIL KUMAR et al., 2010).

The intra-particle diffusion model is used to determine the rate limiting step of the adsorption kinetics. Also known as the Weber-Morris model the intra-particle diffusion model can be describe as presented on Equation 4 (WEBBER, MORRIS; 1963).

$$q_t = k_{IPD}t^{1/2} + C \tag{4}$$

Where k_{IPD} (mg/g $min^{1/2}$) is the rate parameter of stage and is obtained from the slope of the straight line of q_t versus $t^{1/2}$ plot. Also, C is the intercept of the linear plot and describes the boundary layer, which means the greater the intercept, the greater the boundary layer effect (LUUKKONEN et al., 2016). If the adsorption process occurs only by intraparticle diffusion, then the q_t versus $t^{1/2}$ plot will be linear and passes through origin. Otherwise, some other mechanism is also involved (TAN; AHMAD; HAMEED, 2009).

2.5.2 Adsorption Isotherms

The experimental of the adsorption equilibrium data were tested through the Freundlich and Langmuir to describe the characteristics of adsorption equilibrium. These adsorption isotherms describe how the adsorbate interacts with the adsorbent. Adsorption isotherms, present a comprehensive understanding of the nature of these interactions. Besides, it can present relevant information related to the optimum usage of the adsorbent.

The Langmuir model assumes that the adsorbent has a constant number of adsorption sites and sorption on adsorbent surface is monolayer and homogeneous (AGRAFIOTI; KALDERIS; DIAMADOPOULOS, 2014). The Langmuir equation can be described as presented in Equation 5 (CHEN, 2015).

$$q_e = \frac{q_m K_L C_e}{1+K_L C_e} \tag{5}$$

The linear form of the Langmuir isotherm equation can be illustrated as presented in Equation 6 (HAN et al., 2014):

$$\frac{C_e}{q_e} = \frac{1}{q_m K_L} + \frac{C_e}{q_m} \quad (6)$$

where C_e (mg/L) is the equilibrium concentration of adsorbate, q_e (mg/g) is the amount of adsorbate adsorbed per unit mass of adsorbent and q_m (mg/g) and K_L (L/mg) are the Langmuir constants related to maximum monolayer adsorption capacity and energy change in adsorption, respectively.

The Freundlich model is the relationship that describes the non-ideal and reversible adsorption, which can be applied to multilayer adsorption, derived by assuming a heterogeneous surface with a non-distribution of heat of adsorption over the surface (KISKU et al., 2015). The Freundlich model is represented by Equation 7 (AGRAFIOTI; KALDERIS; DIAMADOPOULOS, 2014).

$$q_e = K_F C_e^{1/n} \quad (7)$$

where q_e (mg/g) is the amount of IC adsorbed per mass of adsorbent and C_e (mg/L) is the concentration of the adsorbate at equilibrium. The equation can be linearized by linear regression represented by Equation 8 (HAN et al., 2014).

$$\ln q_e = \ln K_F + \frac{1}{n} \ln C_e \quad (8)$$

where K_F and 1/n are Freundlich constants which correspond to maximum adsorption capacity and strength of adsorption, respectively.

Temkin isotherm takes into consideration the adsorbent-adsorbate interactions, assuming that the heat of adsorption decreases linearly with increasing coverage. The Temkin isotherm is expressed by Equation 9 and 10 (DADA et al., 2012).

$$q_e = B \ln A_T + B \, lnC_e \quad (9)$$

$$B = \frac{RT}{b} \quad (10)$$

where A_T is the Temkin isotherm constant at equilibrium corresponding to the maximum biding energy (L/g), B is the heat of adsorption (J/mol), R is the universal gas constant (8.314 J/molK), T is the absolute temperature, b is the Temkin isotherm constant, which indicates the adsorption potential of the adsorbent. Both A_T and B can be determined from a plot of q_e versus lnC_e and the constants were determined from the intercept and slope, respectively (DEHGHANI et al., 2016).

3 MATERIALS AND METHODS

3.1 Materials

The RHA was provided by a rice mill industry *Arroz Fumacense Ltda, Morro da Fumaça*, *SC*, Brazil produced by burning the rice husk for energy production to its own process. The CR was provided by *Angelgres* located in *Criciúma*, *SC*, Brazil. This residue is generated after the process of forming the pieces before passing through the drying ovens, from defective pieces and from the material that no longer can be reincorporated into the production process.

Both residues were dry-milled in alumina ball mill and sieved before use. The particle size distribution was measured and the average size (D_{50}), to RHA and ceramic residue were 0,227 μm and 0,591 μm, respectively.

The chemical composition (major elements) of materials were determined by a Panalytical Axios X-ray fluorescence spectrometer. Table 1 shows the chemical composition from both residues.

Table 1 – Chemical characterization for rice husk ash (RHA) and ceramic residue (CR).

Sample	**Oxides (%)**										
	Al_2O_3	**CaO**	**Fe_2O_3**	**K_2O**	**MgO**	**MnO**	**Na_2O**	**P_2O_5**	**SiO_2**	**TiO_2**	**LOI**
RHA	0,13	0,44	0,16	0,76	0,38	0,09	0,07	0,7	70,75	<0,05	26,47
CR	10,87	9,2	0,8	2,09	3,76	<0,05	2,89	0,29	57,91	0,42	11,7

Source: adapted from COLELLA et al, 2017

Sodium hydroxide 98.81% purity from Neon was used as the alkaline activator. The NaOH solution 9M was prepared utilizing sodium hydroxide pellets, which were dissolved in distilled water. The solution was used when reached room temperature.

The IC used is from Neon and it was utilized without any further treatment or any other pre-treatment process. Its chemical formula is $C_{16}H_8N_2Na_2O_8S_2$ and has a molecular weight of 466.35 g/mol.

3.2 Methods

3.2.1 Geopolymer synthesis

The formulation of the geopolymeric paste were prepared varying the mass ratios of RHA and CR, and fixing the solid-liquid ratio 0.83 (g/g) as presented on Table 2.

Table 2 – Percent mass ratios used in CR+RHA-based geopolymer synthesis.

Sample	RHA (g)	CR (g)	CR (w%)	NaOH (M)	Water mass fraction (g/g)
T1	150	0	0%	9	0.83
T2	112.5	37.5	25%	9	0.83
T3	75	75	50%	9	0.83
T4	37.5	112.5	75%	9	0.83

Source: COLELLA et al, 2017

For the geopolymer synthesis both solid residues were mixed first for one minute in low velocity, and then the 9M NaOH solution was added during one minute and lastly, both liquid and solids were vigorously stirred for 8 more minutes, totalizing 10 minutes for the synthesis of the geopolymeric paste at ambient temperature (approximately 298K). Geopolymer pastes were cast into a Polyvinyl chloride cylinder mold of 20 mm diameter and 40 mm height, vibrated for 5 min to release the bubbles and cured at 50 °C, being unmolded after 5 days and returned to oven at same temperature for more 7 days. And then it was kept at room temperature until completion of 28 days. Figure 6 shows a schematic design for the geopolymer synthesis.

Figure 6 – Geopolymer formation process.

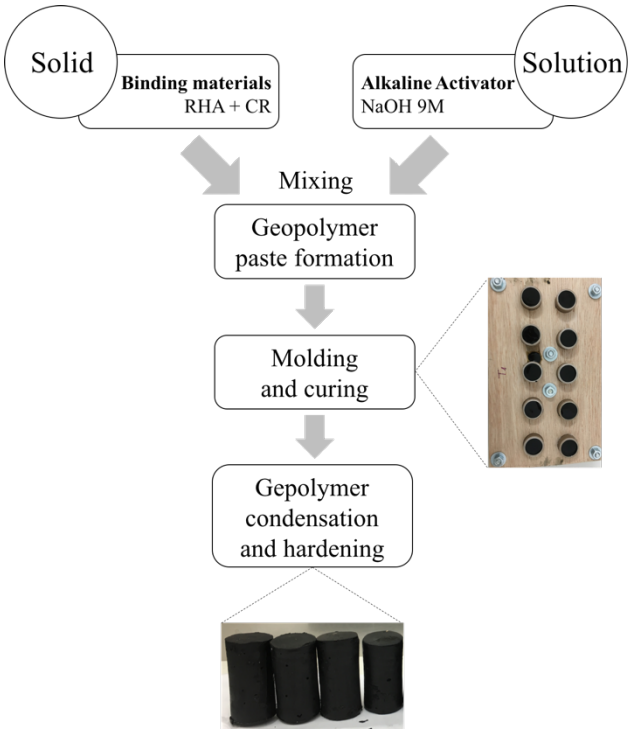

Source: author.

Morphology analysis of the geopolymers was performed using scanning electron microscopy (SEM – Hitachi, TM3030) images and energy dispersive X-ray spectroscopy operated at 15 kV. Also, the porosity of the geopolymer was calculated in triplicate using the ImageJ® software with the Huang filter of the SEM images previously done by Colella *et al*, 2017.

3.2.2 Batch adsorption experiments

To adsorption experiment a stock solution of IC 1(000 mg/L) in water was prepared. An absorbance scan from 580 to 630 nm was performed in order to determine the wavelength of maximum absorbance at this interval, using an IC solution of 20 mg/L by Thermo Scientific Genesys 6 UV-Vis.

Concentration calibration curves according to the Lambert-Beer law were established at λ=610 nm by measuring the UV absorbance (*A*) of solutions with a known concentration of IC (5, 10, 15, 20 and 25) at room temperature where the dye concentration is in mg/L. Examples of the solutions used at the calibration curve are shown in Figure 7.

Figure 7 – Dye solutions in concentrations of 5, 10, 15, 20 and 25 mg/L from the left to the right.

Source: author.

3.2.3 Batch adsorption experiments

The batch adsorption experiments were conducted in duplicate with an initial pH of 8.5 and a set of 250 mL of Erlenmeyer flask containing solutions with 50 mL of IC with various initial concentrations. The flasks were agitated in an isothermal shaker at 120 rpm until the equilibrium was reached. After adsorption test the solution was centrifuged in a Centrífuga Excelsa II Modelo 206-BL FANEM for 10 min and 3500 rpm, the equilibrium concentrations of dye in the solution were measured at 610 nm using UV-visible spectrophotometer.

The percentage removal of IC (Y) and the adsorption capacity q (mg/g) were calculated from Equations 11 and 12. Where V (L) is the experimental volume, m (g) the mass of the adsorbent, C_0 (mg/L) the initial concentration of the dye solution and C_e (mg/L) the equilibrium concentration.

$$q = \left(\frac{C_0 - C_e}{m}\right).V \tag{11}$$

$$Y = \left(\frac{C_0 - C_e}{C_0}\right).100\% \tag{12}$$

3.2.4 Adsorbent dose

In order to assess the effect of adsorbent dose (m, in g), several adsorbent doses were tested. The concentrations used were: 0.01, 0.04, 0.08, 0.16 and 0.32 g/mL (mass of geopolymer adsorbent per volume of IC solution). Temperature was fixed at 298K, the contact time 120 minutes and initial concentration of IC 50 mg/L. After adding the adsorbent into the IC solution, an incubator was used to homogenously mix the solutions in a controlled environment.

3.2.5 Adsorption kinetics

After having the optimum adsorbent dose, the next step was to determine the optimum contact time between the adsorbent and the adsorbate at a fixed temperature of 298K. The solutions were prepared in a 125 mL Erlenmeyer, using the 25, 50 and 75 mg/L of the IC solutions in six different contact times 5, 10, 20, 30, 60 and 120 minutes and with the optimum dose of adsorbent determined in the previous test. Figure 8 shows an example of the solutions used for this experiment.

Figure 8 – Example of the solution for the adsorption kinetic experiment.

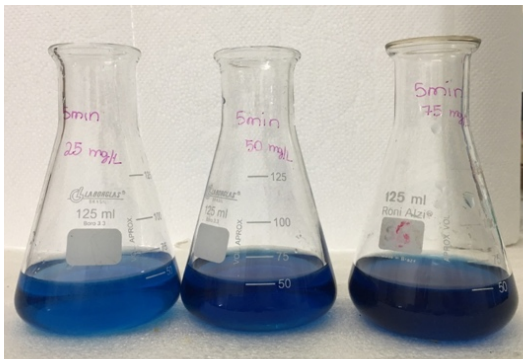

Source: author.

Parameters of the kinetic models were estimated from the experimental data with the aid of the nonlinear curve-fitting procedure. Three kinetic models were used, including pseudo-first-order, pseudo-second-order and intra-particle diffusion models. These models are most commonly used to describe the sorption of dyes as well as other pollutants (heavy metals) on solid sorbents.

3.2.6 Adsorption isotherm studies

The equilibrium isotherms are critical for designing adsorption systems and explaining the surface properties. The adsorption isotherm provides information about distribution of the adsorbed molecules/ions between the liquid and solid phases at equilibrium and explains the relationship between the amount of adsorbate adsorbed onto the adsorbent and the amount remaining in solution at a fixed temperature (ŞAHAN; EROL; YILMAZ, 2018).

After finding the optimum dose adsorbent and the optimum contact time it was possible to determine the influence of the temperature to reach the equilibrium. It was used six different IC concentrations: 15, 25, 35, 50 and 65 mg/L and four temperatures: 298, 303, 313 and 323K.

4 RESULTS AND DISCUSSION

4.1 Geopolymer characterization

Figure 9 shows the micromorphological features of the geopolymer. It can be seen that there are some undissolved particles and some plaques, that can be related to the sample preparation for the characterization. The SEM images show that the geopolymer is a porous material which corroborates for the adsorption to take place and it is believed that adsorption capacity depends on the porous structure and their surface properties. Higher surface area will generally result in higher adsorption capacity (LI; WANG; ZHU, 2006). The porosity was calculated using the ImageJ® software and it was found that the geopolymer porosity is 15.99% with a standard deviation of 0.01.

Figure 9 – SEM of the geopolymer a) zoom x500 b) zoom x1.5k

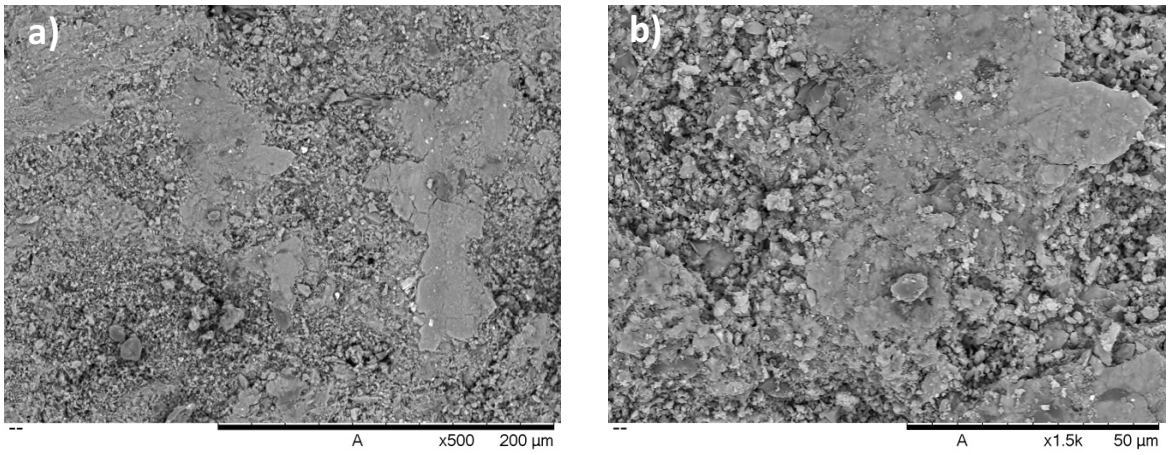

Source: Colella *et al*, 2017.

4.2 Effect of the adsorbent dosage

The UV absorbance of the IC solution (20 mg/L) was analyzed to determine the region where the maximum absorbance occurs. As shown in Figure 10, the IC optimum absorbance wavelength was found to be at 610 nm. This wavelength was, then, used for all the next analyses.

Figure 10 –Absorbance wavelength of IC.

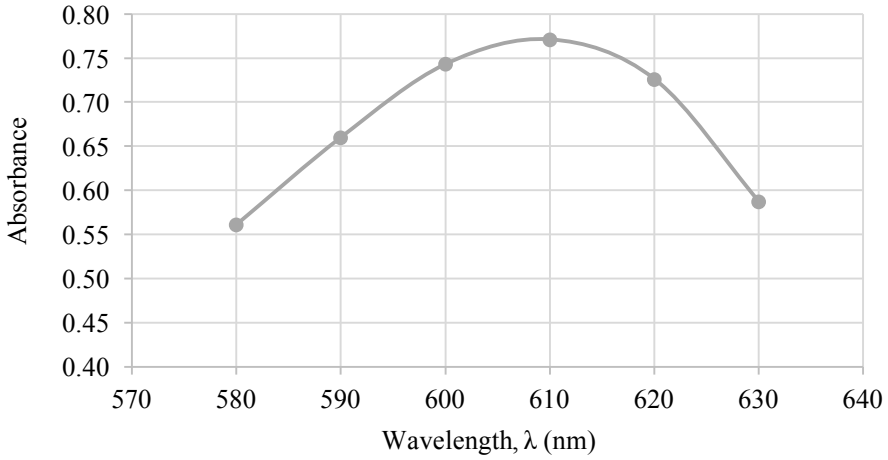

Source: author.

From the concentration and absorbance data, in the wavelength of 610 nm, it was developed the calibration curve. Since concentration and absorbance are proportional, Beer's Law makes it possible to determine an unknown concentration of IC after the adsorption process after determining the absorbance, so we could calculate de the adsorption capacity q (mg/g) and the IC (Y) removal percentage of the Figure 11 represents the calibration curve for the wavelength determined previously. The trend line was determined using Excel, and the Equation 12 is given bellow, and the correlation coefficient (R^2) is equal to 0.9960 which shows the experiment can be represented with great agreement.

$$\%\, Absorbance_{IC} = 0.0395\, C_{IC} \tag{13}$$

Figure 11 – Calibration curve of IC absorbance.

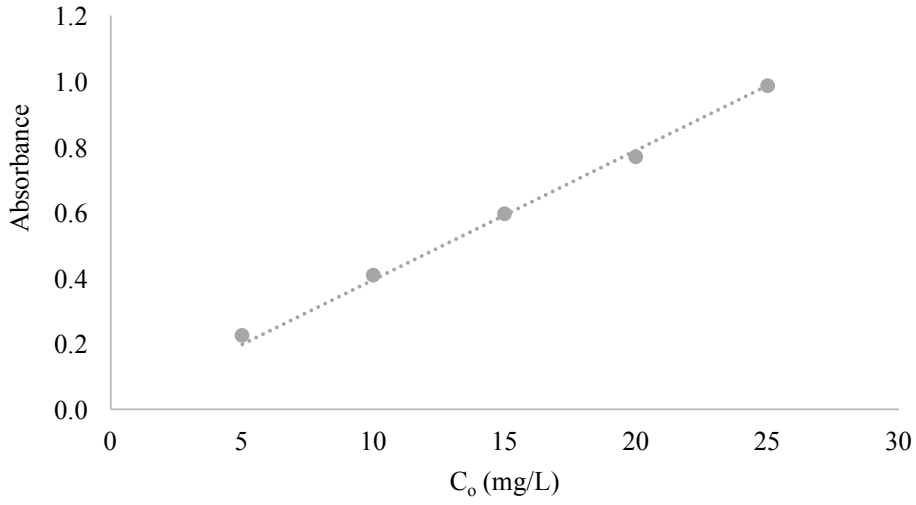

Source: author.

The effect of adsorbent dose at initial concentration $C_o = 50\ mg/L$ and $t = 120\ min$ is shown in Figure 12. The study shows a significant increase on the IC adsorption when the dose of geopolymer was increased from 0.01 to 0.04 g/mL. The optimum geopolymer adsorbent dose was found to be at 0.04 g/mL, since the percentage removal was 100%. After that point, it can be seen that the IC removal remains almost constant. A similar result was found by Senthil et al (2010), stating an increase in the adsorption with an increase in the adsorbent dose can be attributed to a greater porosity and surface area of rice husk ash-based geopolymer, and the availability of more adsorption sites.

Figure 12 – Optimum adsorbent dose (T = 298K, $t = 120\ min$, $C_o = 50\ mg/L$).

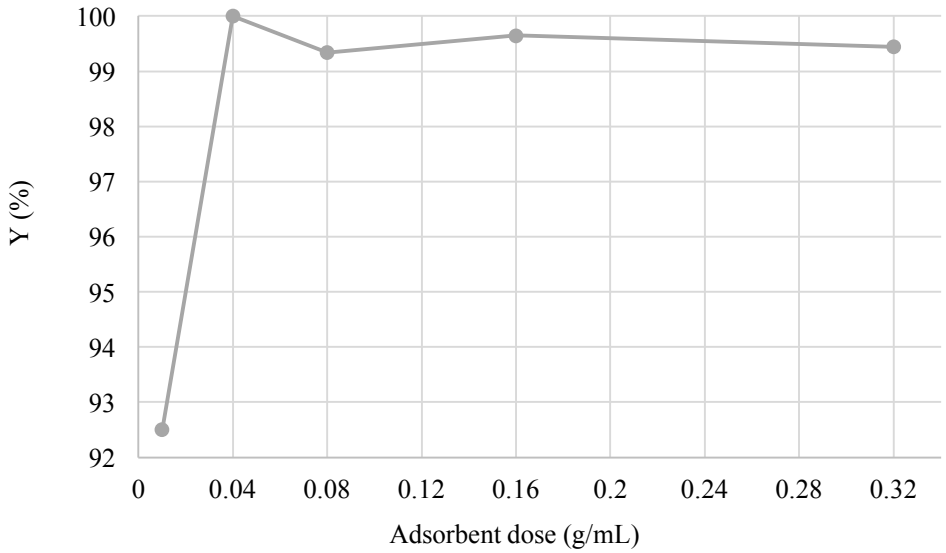

Source: author.

4.3 Effect of contact time (t) and initial IC dye concentration (C_o)

The effect of contact time on the removal of IC at C_o from 25 up to 75 mg/L is given in Figure 13. The contact time curves show that the adsorption is initially fast during the first 10 minutes and then becomes progressively slower as the contact time increases, reaching the equilibrium in 60 minutes. This was explained in other studies (ARENAS et al., 2017; LAKSHMI et al., 2009) stating that dye molecules can aggregate with time and therefore is harder for the diffusion to occur. Besides, the pores of the geopolymer could be saturated and, then start offering a resistance to the adsorption process.

Figure 13 – Effect of contact time on the percentage removal of IC and the adsorption capacity (T = 298K, $m = 2\ g$).

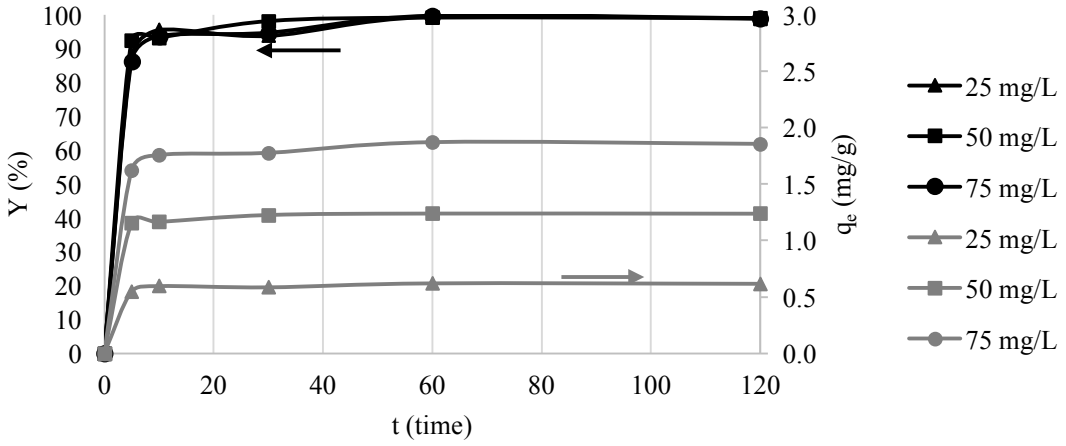

Source: author.

As already expected and shown in Figure 13, the adsorption capacity q_e at equilibrium increase from 0.62 to 1.8 mg/g, with an increase in the initial dye concentration C_0 from 25 to 75 mg/L. However, no significant changes in removal efficiency were observed, for all concentrations it was approximately 99% at 60 min. Similar trend was obtained in the adsorption of IC on materials RHA based (ARENAS et al., 2017).

4.4 Kinetic studies

Since kinetic models are exploited to test the experimental data it is important to be able to predict the rate at which contamination is removed from aqueous solutions in order to design an adsorption treatment process and to understand the controlling mechanism of adsorption and its potential rate-controlling steps that include mass transport and chemical reaction processes.

In this study, the experimental equilibrium data of IC onto RHA and CR-based geopolymer was first analyzed by the pseudo-first-order, pseudo-second-order kinetic and intraparticle diffusion models (Table 3 and Table 4). Table 3 present the results of fitting experimental data with pseudo-first-order and pseudo-second-order models using correlation coefficient (R^2) and Table 4 present the results of fitting experimental data with intraparticle diffusion model. A comparison of the error functions indicates that the pseudo-first-order and intraparticle diffusion equation can not provide an accurate fit of the experimental data, exhibited a correlation coefficient (R^2) lower than unity 0.40, 0.78, 0.56 when C_o was 25, 50 e

50 mg/L, respectively. The results suggest that pseudo-second-order kinetic model, in contrast to the pseudo-first-order model and intraparticle diffusion, provided a good correlation for the adsorption of IC on RHA and CR-based geopolymer and that adsorption reaction onto the surface of adsorbent is the rate- controlling step.

From Table 3 it can be seen that the values of the rate constant K_{PSO} decrease as the initial concentration increases. At lower concentrations, this behavior can be attributed to the lower competition for the sorption surface sites. At higher concentrations, the competition for the surface active sites will be higher and therefore lower sorption rates are obtained (SENTHIL KUMAR et al., 2010).

Table 3 – Kinetic parameters calculated according pseudo-first order and pseudo-second order model at 298K.

C_o [mg/L]	Pseudo-first Order			Pseudo-second Order		
	K_{PFO} [min^{-1}]	q_e [mg/g]	R^2	K_{PSO} [g/mg min]	q_e [mg/g]	R^2
25	0.032	0.458	0.404	2.903	0.621	0.999
50	0.056	0.682	0.781	2.534	1.242	0.999
75	0.036	0.806	0.562	0.935	1.866	0.999

Source: author.

Also, it can be observed from Table 4 that the C value increase with increasing IC initial concentrations, meaning that the boundary layer diffusion mechanism becomes more significant when the dye concentration increases (CARVALHO et al., 2011).

Table 4 – Kinetic parameters calculated according intraparticle diffusion model at 298K.

C_o [mg/L]	Intraparticle diffusion model		
	K_{IPD} [$mg/g.min^{1/2}$]	C [mg/g]	R^2
25	0.007	0.555	0.639
50	0.010	1.144	0.774
75	0.024	1.634	0.720

Source: author.

In Figure 14 the intercept of the straight line plots of $\log(q_e - q_t)$ versus t shloud be equal to $log\ q_e$. However, if the intercept is not equal to q_t, then the reaction is not likely to be a first order reaction, moreover this plot has high determination coefficient with the experimental data (CARVALHO et al., 2011; HO; MCKAY, 1999). As also seen in Table 3, q_e values did not agree with the calculated ones obtained from the linear plots, indicating that the pseudo-first order model does not represent the adsorption kinetics of IC onto the

geopolymer. Many other studies have shown similar results (BALARAK et al., 2015; DASTKHOON et al., 2018; ENAIME et al., 2017; ZHANG; ZHOU; OU, 2016). Figure 13 shows the linear approximation for the pseudo-first order model.

Figure 14 - Pseudo-first order kinetic fit for adsorption IC into geopolymer at 298K

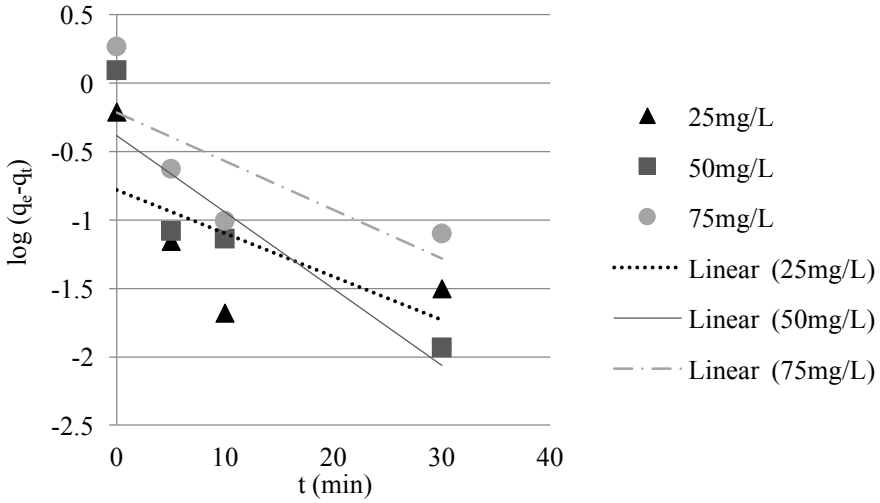

Source: author.

Figure 15 presents the linear plot of t/q_t versus t and shows a good agreement between the experimental data and the calculated q_e. Also, the correlation coefficient shows it is very close to unit, therefore the sorption process can be approximated more accurately by the pseudo-second order kinetic model.

Figure 15 – Pseudo-second order kinetic fit for adsorption IC into geopolymer at 298K.

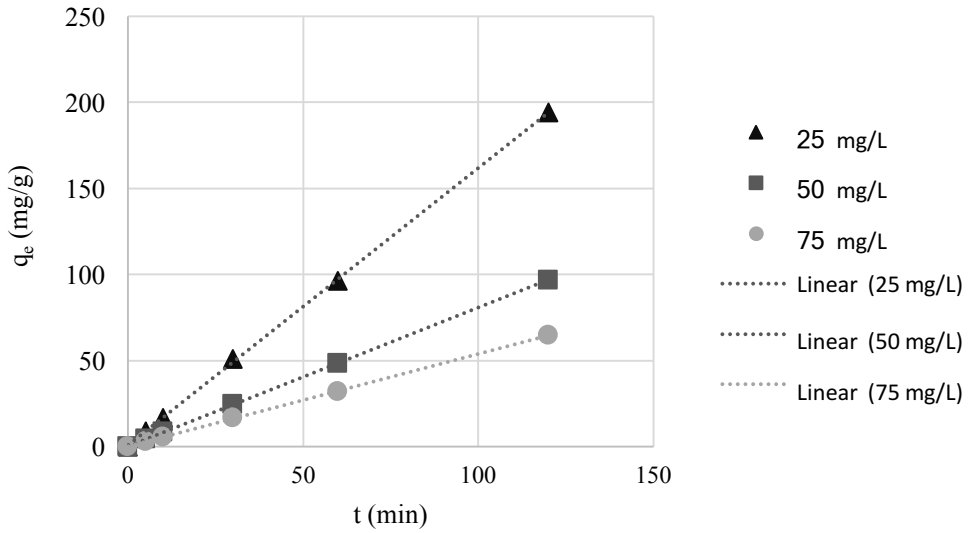

Source: author.

Figure 16 shows the plot of q_t versus $t^{1/2}$ for intraparticle diffusion model. The linear plots at each concentration did not pass through the origin, indicating that the intraparticle diffusion was not the only rate-limiting mechanism (SENTHIL KUMAR et al., 2010). This pattern could be related to the wide distribution of pore size of the geopolymer, consequently, more than one process is taking place in the adsorption process (ARENAS et al., 2017; WU; TSENG; JUANG, 2009).

Figure 16 – Intraparticle diffusion model kinetic fit for adsorption IC into geopolymer at 298K.

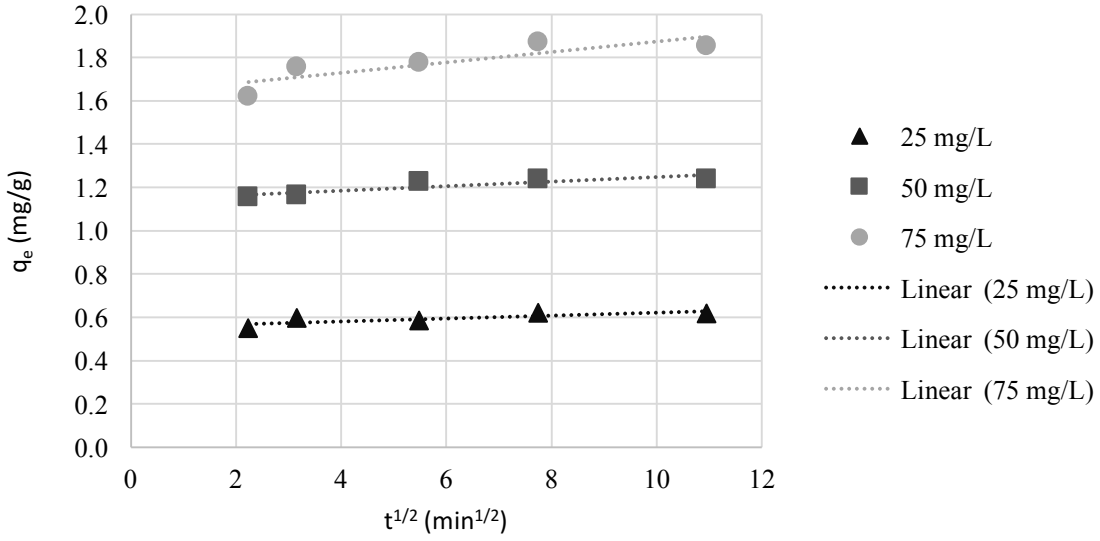

Source: author.

4.5 Effect of temperature

4.5.1 Temperature effect on the adsorption capacity

In order to investigate the effect of temperature on the adsorption onto geopolymer, removal of IC experiments were carried out at different temperatures. The relationship between the temperature and the adsorption capacity values is illustrated in Figure 17. Adsorption capacities of geopolymer based on RHA and CR for IC slightly increased from 0.35 to 0.36 mg/g for the lowest initial concentration of IC (15 mg/L) and 1.24 to 1.35 mg/g for highest initial concentration of IC (65 mg/L), respectively when the temperature was increased from 298 to 323K. As shown in Figure 17, adsorption capacities were not significantly affected by the temperature after 298K. This could be evaluated as an important advantage since at the operational cost of the process increases at higher temperatures (KARA; YILMAZER; AKAR, 2017). Therefore, further adsorption studies were conducted at 298K.

Figure 17 – Effect of temperature on the adsorption capacity.

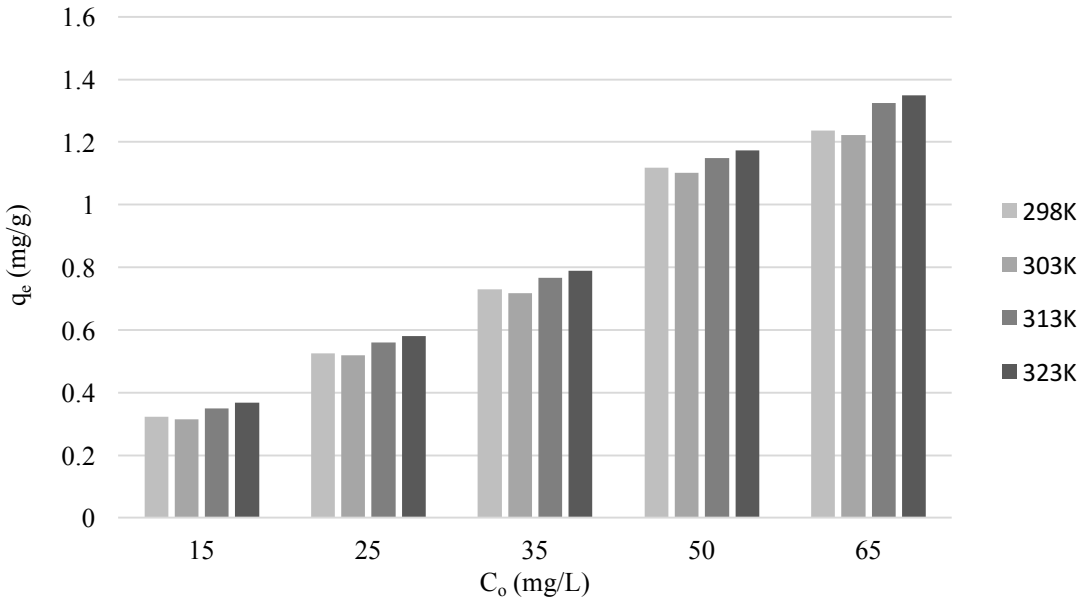

Source: author.

4.5.2 Effect of temperature on the percentage removal of IC

Also, it was evaluated the effect of temperature on the percentage removal of IC from aqueous solution, shown in Figure 18. Although the effect of temperature on adsorption capacity is not significant, it can be seen from Figure 18 that the percentage removal is really affected on the percentage removal of IC. At the slowest concentration (15 mg/L) the percentage removal increased from 84% to 96% when the temperature was increased from 298 to 323K. For the highest concentration (65 mg/L) percentage removal increased from 90% to 98% for the same temperature range. And this behavior can be observed for all concentrations.

The adsorption is an exothermic process and hence, an increase in the solution temperature must result in a decrease in the sorption capacity (ARENAS et al., 2017). Nevertheless, the diffusion process is considered an endothermic process and therefore, if the adsorption process along the reaction time is controlled in some extent by intra-particle diffusion steps, the adsorption capacity must show an increase with temperature. An increase in the solution temperature could lead to an increase of the IC ions mobility and the retarding forces acting on the diffusing ions could also decrease. This pattern can explain the increase of the adsorption capacity of RHA and CR-based geopolymer material.

Figure 18 – Effect of temperature on percentage removal of IC.

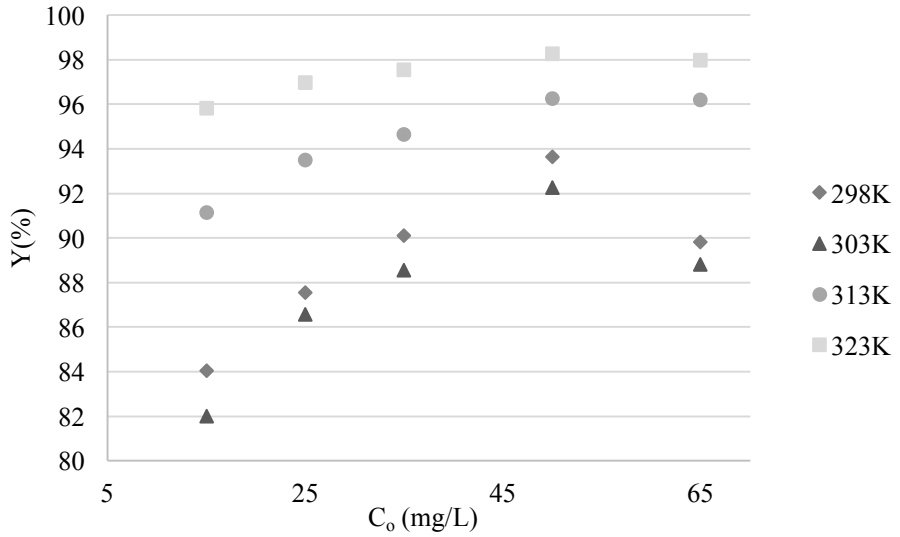

Source: author.

4.6 Adsoprtion isotherms

The respective parameters for each model and its correlation coefficient (R^2) are reported in Table 5, which shows that Langmuir models do not describe properly the adsorption process of IC dye onto RHA and CR-based geopolymer since all correlation coefficients are far from unit. While the Freundlich isotherm show better fitting to describe adsorption on RHA and CR-based geopolymer indicate that surface having heterogeneous energy distribution accompanied by interaction between the adsorbed molecules and adsorbate.

The detailed analysis of the correlation coefficient values showed that the Temkin model fit the adsorption data better than the Langmuir model at different temperature. This isotherm contains a factor that explicitly takes into the account of adsorbent–adsorbate interactions. If we disconsider the extremely low and large value of concentrations, the model assumes that heat of adsorption (function of temperature) of all molecules in the layer would decrease linearly rather than logarithmic with coverage.

Table 5 – Isotherms parameters.

Temperature	Langmuir			Freundlich			Temkin		
(K)	q_m (mg/g)	K_L (L/mg)	R^2	n	K_F (L^{-1})	R^2	B_T	K_T (L/mg)	R^2
298	2.155	0.070	0.101	0.743	0.140	0.572	0.973	0.678	0.613
303	1.461	0.082	0.205	0.650	0.090	0.694	0.093	0.001	0.741
313	0.321	0.402	0.811	0.314	0.140	0.924	2.355	0.840	0.908
323	0.616	0.662	0.523	0.435	1.243	0.819	1.814	1.973	0.864

Source: author.

5 CONCLUSION

Batch adsorption removal of IC from aqueous solution onto the geopolymer was investigated under different conditions. The most favorable condition had with a 99% percentage removal with an adsorbent dose level of 0.04 g/mL in the IC concentration of 50 mg/L and a contact time of 60 minutes. The kinetic studies showed correlation coefficient closer to unit for the pseudo-second. Therefore, the sorption process can be described more accurately by the pseudo-second order model for all initial concentrations. The effect of temperature on adsorption capacity was studied and the results showed that it had a slightly increase from 0.35 to 0.36 mg/g for the lowest initial concentration of IC (15 mg/L) and 1.24 to 1.35 mg/g for highest initial concentration of IC (65 mg/L). The effect of temperature on the percentage removal was also studied. At the slowest concentration (15 mg/L) the percentage removal increased from 84% to 96% when the temperature was increased from 298 to 323K. The equilibrium adsorption data was adequately represented by Freundlich and Temkin adsorption models. The maximum adsorption capacity for IC was found to be 1.35 mg/g at T = 323 K with an initial concentration of 65 mg/L. To sum up, the study showed a promising low cost adsorbent to be used in the removal of IC from aqueous solutions.

REMOÇÃO DE INDIGO CARMINE UTILIZANDO GEOPOLÍMERO DA CINZA DA CASCA DE ARROZ COMO ADSORVENTE

RESUMO

A remoção por adsorção de Indigo Carmine (IC) de soluções aquosas utilizando um geopolímero sintetizado a partir de dois resíduos industriais, a cinza da casca de arroz (RHA) e o resíduo cerâmico (CR), foi investigada sob diferentes condições. Verificou-se que a condição mais favorável para dose de adsorvente foi de 0,04 g/mL na concentração de 50 mg/L e um tempo de contato de 60 minutos. A remoção percentual nas concentrações iniciais de IC para 50 mg/L foi de aproximadamente 99%. Os estudos cinéticos mostraram que o processo de adsorção segue o modelo de Pseudo-Segunda ordem. O efeito da temperatura sobre a capacidade de adsorção e o pecentual de remoção de IC também foi estudado. Finalmente, os dados de adsorção em equilíbrio foram bem representados pelos modelos de adsorção de Freundlich e Temkin. A capacidade máxima de adsorção para IC foi de 1,35 mg/g para a temperatura de 323K com uma concentração inicial de 65 mg/L. Portanto, a partir dos resultados, esse geopolímero pode ser utilizado como adsorvente para a remoção de Indigo Carmine de água contaminadas das indústrias têxteis.

Palavras-chave: Indigo Carmine, Geopolímero, Cinza da Casca de Arroz, Adsorção.

REFERÊNCIAS

AGRAFIOTI, E.; KALDERIS, D.; DIAMADOPOULOS, E. Arsenic and chromium removal from water using biochars derived from rice husk , organic solid wastes and sewage sludge. **Journal of Environmental Management**, v. 133, p. 309–314, 2014.

AGUIRRE-GUERRERO, A. M.; ROBAYO-SALAZAR, R. A.; DE GUTIÉRREZ, R. M. A novel geopolymer application: Coatings to protect reinforced concrete against corrosion. **Applied Clay Science**, v. 135, p. 437–446, 2017.

AHMED, M. J. K.; AHMARUZZAMAN, M. A review on potential usage of industrial waste materials for binding heavy metal ions from aqueous solutions. **Journal of Water Process Engineering**, v. 10, p. 39–47, 2016.

AL-HARAHSHEH, M. S. et al. Fly ash based geopolymer for heavy metal removal: A case study on copper removal. **Journal of Environmental Chemical Engineering**, v. 3, n. 3, p. 1669–1677, 2015.

AL-ZBOON, K.; AL-HARAHSHEH, M. S.; HANI, F. B. Fly ash-based geopolymer for Pb removal from aqueous solution. **Journal of Hazardous Materials**, v. 188, n. 1–3, p. 414–421, 2011.

ALI, I.; GUPTA, V. K. Advances in water treatment by adsorption technology. **Nature Protocols**, v. 1, n. 6, p. 2661–2667, 2007.

AMMAR, S. et al. Electrochemical degradation of the dye indigo carmine at boron-doped diamond anode for wastewaters remediation. **Original Paper**, v. 4, p. 229–233, 2006.

ARENAS, C. N. et al. Removal of Indigo Carmine (IC) from aqueous solution by adsorption through abrasive spherical materials made of rice husk ash (RHA). **Process Safety and Environmental Protection**, v. 106, p. 224–238, 2017a.

ARENAS, C. N. et al. Removal of Indigo Carmine (IC) from aqueous solution by adsorption through abrasive spherical materials made of rice husk ash (RHA). **Process Safety and Environmental Protection**, n. Ic, 2017b.

ARIFFIN, N. et al. Geopolymer as an adsorbent of heavy metal: A review. **AIP Conference Proceedings**, v. 1885, 2017.

AWOYERA, P. O. et al. Characterization of ceramic waste aggregate concrete. **HBRC Journal**, p. 1–6, 2016.

BAKHAREV, T. Thermal behaviour of geopolymers prepared using class F fly ash and elevated temperature curing. **Cement and concrete research**, v. 36, p. 1134–1147, 2006.

BALARAK, D. et al. The use of low-cost adsorbent (Canola residues) for the adsorption of methylene blue from aqueous solution: Isotherm, kinetic and thermodynamic studies. **Colloids and Interface Science Communications**, v. 7, p. 16–19, 2015.

CARVALHO, T. DE et al. Adsorption of indigo carmine from aqueous solution using coal fly ash and zeolite from fly ash. **J Radioanal Nucl Chem**, v. 289, p. 617–626, 2011.

CASASOLA, R.; RINCÓN, J. M.; ROMERO, M. **Glass-ceramic glazes for ceramic tiles: A reviewJournal of Materials Science**, 2012.

CHEN, X. Modeling of Experimental Adsorption Isotherm Data. **Information**, n. 6, p. 14–22, 2015.

CHOWDHURY, A. K.; SARKAR, A. D.; BANDYOPADHYAY, A. Rice Husk Ash as a Low Cost Adsorbent for the Removal of Methylene Blue and Congo Red in Aqueous Phases. **Clean Journal**, v. 37, n. 7, p. 581–591, 2009.

COLELLA, J et al. Production of geopolymer from industrial wastes. 61˚ Congresso Brasileiro de Cerâmica (61 CBC), 2017.

CONAB – Companhia Nacional de Abastecimento. **Acompanhamento safra brasileira grãos, v.12 Safra 2015/16** – Décimo Segundo levantamento, Brasília, p. 1-182, setembro 2016.

DADA, A. . et al. Langmuir, Freundlich, Temkin and Dubinin–Radushkevich Isotherms Studies of Equilibrium Sorption of Zn 2+ Unto Phosphoric Acid Modified Rice Husk. **IOSR Journal of Applied Chemistry**, v. 3, n. 1, p. 38–45, 2012.

DAIFULLAH, A. A. M.; GIRGIS, B. S.; GAD, H. M. H. Utilization of agro-residues (rice husk) in small waste water treatment plans. **Materials Letter**, v. 57, p. 1723–1731, 2003.

DASTKHOON, M. et al. Synthesis of CuS nanoparticles loaded on activated carbon composite for ultrasound-assisted adsorption removal of dye pollutants: Process optimization using CCD-RSM, equilibrium and kinetic studies. **Applied Organometallic Chemistry**, n. November 2017, p. 1–11, 2018.

DAVIDOVITS, J. GEOPOLYMERS Inorganic polymerie new materials. **Journal of Thermal Analysis**, v. 37, p. 1633–1656, 1991.

DAVIDOVITS, J. Eopolymer Cement. **Institut Géopolymere**, n. 0, p. 1–11, 2013.

DEHGHANI, M. H. et al. Removal of chromium(VI) from aqueous solution using treated waste newspaper as a low-cost adsorbent: Kinetic modeling and isotherm studies. **Journal of Molecular Liquids**, v. 215, p. 671–679, 2016.

DUXON, P. et al. Geopolymer technology : the current state of the art. **J Mater Sci**, v. 42, n. 4, p. 2917–2933, 2007.

ENAIME, G. et al. Preparation and characterization of activated carbons from olive wastes by physical and chemical activation : Application to Indigo carmine adsorption. v. 8, n. 11, p. 4125–4137, 2017.

FENG, Q. et al. Adsorption of lead and mercury by rice husk ash. **Journal of Colloid and Interface Science**, v. 278, p. 1–8, 2004.

FOO, K. Y.; HAMEED, B. H. Utilization of rice husk ash as novel adsorbent : A judicious recycling of the colloidal agricultural waste. **Advances in Colloid and Interface Science**, v. 152, n. 1–2, p. 39–47, 2009.

FAOSTAT – Food and agriculture organization of the United Nations Statistics. Available on: http://faostat.fao.org. Accessed on: 14/05/2017.

GEORGIEVA, V. G. et al. Adsorption kinetics of Cr(VI) ions from aqueous solutions onto black rice husk ash. **Journal of Molecular Liquids**, v. 208, p. 219–226, 2015.

HAN, K. et al. Adsorption isotherms and kinetics of cationic and anionic dyes on three-dimensional reduced graphene oxide macrostructure. **Journal of Industrial and Engineering Chemistry**, p. 1–6, 2014.

HO, Y. S.; MCKAY, G. Pseudo-second order model for sorption processes. **Process Biochemistry**, v. 34, n. 5, p. 451–465, 1999.

HU, Y. et al. Activated carbon doped with biogenic manganese oxides for the removal of indigo carmine. **Journal of Environmental Management**, v. 166, p. 512–518, 2016.

HUANG, Y.; HAN, M. The influence of Al2O3 addition on microstructure , mechanical and formaldehyde adsorption properties of fly ash-based geopolymer products. **Journal of Hazardous Materials**, v. 193, p. 90–94, 2011.

KAMATH, S. R.; PROCTOR, A. Silica Gel from Rice Hull Ash: Preparation and Characterization. **Cereal Chem.**, v. 75, n. 4, p. 484–487, 1998.

KARA, İ.; YILMAZER, D.; AKAR, S. T. Metakaolin based geopolymer as an effective adsorbent for adsorption of zinc(II) and nickel(II) ions from aqueous solutions. **Applied Clay Science**, v. 139, p. 54–63, 2017.

KISKU, G. C. et al. Characterization and adsorptive capacity of coal fly ash from aqueous solutions of disperse blue and disperse orange dyes. **Environ Earth Sci**, 2015.

KUMAR, T. et al. The sorption of lead (II) ions on rice husk ash. **Journal of Hazardous Materials**, v. 163, p. 1254–1264, 2009.

LABIADH, L. et al. Direct and indirect electrochemical oxidation of Indigo Carmine using PbO2 and TiRuSnO2. **J Solid State Eletrochem**, 2017.

LAKSHMI, U. R. et al. Rice husk ash as an effective adsorbent : Evaluation of adsorptive characteristics for Indigo Carmine dye. **Journal of Environmental Management**, v. 90, n. 2, p. 710–720, 2009.

LI, L.; WANG, S.; ZHU, Z. Geopolymeric adsorbents from fly ash for dye removal from aqueous solution. **Journal of Colloid and Interface Science**, v. 300, p. 52–59, 2006.

LIANG, C. et al. Treatment of highly concentrated wastewater containing multiple synthetic dyes by a combined process of coagulation / flocculation and nanofiltration. **Journal of Membrane Science**, v. 469, p. 306–315, 2014.

LIEW, Y. M. et al. Structure and properties of clay-based geopolymer cements: A review. **Progress in Materials Science**, v. 83, p. 595–629, 2016.

LUUKKONEN, T. et al. Metakaolin geopolymer characterization and application for ammonium removal from model solutions and landfill leachate. **Applied Clay Science**, v. 119, p. 266–276, 2016.

MAJIDI, B. Geopolymer technology, from fundamentals to advanced applications : a review. **Materials Technology**, v. 24, n. 2, p. 79–87, 2009.

MARASENI, T. N. et al. An international comparison of rice consumption behaviours and greenhouse gas emissions from rice production. **Journal of Cleaner Production**, v. 172, p. 2288–2300, 2018.

MITTAL, A.; MITTAL, J.; KURUP, L. Batch and bulk removal of hazardous dye, indigo carmine from wastewater through adsorption. **Journal Hazardous Materials**, v. 137, p. 591–602, 2006.

NACIRI, N. et al. Effective photocatalytic decolorization of indigo carmine dye in Moroccan natural phosphate – TiO2 aqueous suspensions. **Optical Materials**, v. 52, p. 38–43, 2016.

OROS, G.; FORGACS, E.; CSERHATI, T. Removal of synthetic dyes from wastewaters : a review. **Environment International**, v. 30, p. 953–971, 2004.

OTHMAN, I.; MOHAMED, R. M.; IBRAHEM, F. M. Study of photocatalytic oxidation of indigo carmine dye on Mn-supported TiO2. **Journal of photochemistry and photobiology**, v. 189, p. 80–85, 2007.

PALMA-GOYES, R. E. et al. Comparative degradation of indigo carmine by electrochemical oxidation and advanced oxidation processes. **Electrochimica Acta**, 2014.

PAZ, A. et al. **Biological treatment of model dyes and textile wastewaters**. [s.l.] Elsevier Ltd, 2017.

PERIĆ, J.; TRGO, M.; VUKOJEVIĆ MEDVIDOVIĆ, N. Removal of zinc, copper and lead by natural zeolite - A comparison of adsorption isotherms. **Water Research**, v. 38, n. 7, p. 1893–1899, 2004.

PRADO, A. G. S. et al. Comparative adsorption studies of indigo carmine dye on chitin and chitosan. **JOURNAL OF COLLOID AND INTERFACE SCIENCE**, v. 277, p. 43–47, 2004.

QUISPE, I.; NAVIA, R.; KAHHAT, R. Energy potential from rice husk through direct combustion and fast pyrolysis : A review. **Waste Management**, v. 59, p. 200–210, 2017.

RAUF, M. A.; ASHRAF, S. S. Fundamental principles and application of heterogeneous photocatalytic degradation of dyes in solution. **Chemical Engineering Journal**, v. 151, p. 10–18, 2009.

ŞAHAN, T.; EROL, F.; YILMAZ, Ş. Mercury(II) adsorption by a novel adsorbent mercapto-modified bentonite using ICP-OES and use of response surface methodology for optimization.

Microchemical Journal, v. 138, p. 360–368, 2018.

SENTHIL KUMAR, P. et al. Adsorption of dye from aqueous solution by cashew nut shell: Studies on equilibrium isotherm, kinetics and thermodynamics of interactions. **Desalination**, v. 261, n. 1–2, p. 52–60, 2010.

SILVESTRE, R. et al. Using ceramic wastes from tile industry as a partial substitute of natural aggregates in hot mix asphalt binder courses. **Construction and Building Materials**, v. 45, p. 115–122, 2013.

SOOD, S. et al. TiO2 quantum dots for the photocatalytic degradation of indigo carmine dye. **Journal of Alloys and Compounds**, 2015.

SRIVASTAVA, C. V.; MALL, D. I.; MISHRA, I. M. Adsorption thermodynamics and isosteric heat of adsorption of toxic metal ions onto bagasse fly ash (BFA) and rice husk ash (RHA). **Chemical Engineering Journal**, v. 132, p. 267–278, 2007.

TAN, I. A. W.; AHMAD, A. L.; HAMEED, B. H. Adsorption isotherms, kinetics, thermodynamics and desorption studies of 2,4,6-trichlorophenol on oil palm empty fruit bunch-based activated carbon. **Journal of Hazardous Materials**, v. 164, n. 2–3, p. 473–482, 2009.

TAVLIEVA, M. P. et al. Kinetic study of brilliant green adsorption from aqueous solution onto white rice husk ash. **JOURNAL OF COLLOID AND INTERFACE SCIENCE**, 2013.

WORCH, E. **Adsorption Technology in Water Treatment**. [s.l: s.n.].

WU, F. C.; TSENG, R. L.; JUANG, R. S. Initial behavior of intraparticle diffusion model used in the description of adsorption kinetics. **Chemical Engineering Journal**, v. 153, n. 1–3, p. 1–8, 2009.

YAGUB, M. T. et al. Dye and its removal from aqueous solution by adsorption: A review. **Advances in Colloid and Interface Science**, v. 209, p. 172–184, 2014.

ZHANG, J.; ZHOU, Q.; OU, L. Removal of indigo carmine from aqueous solution by microwave-treated activated carbon from peanut shell. **Desalination and Water Treatment**, v. 57, n. 2, p. 718–727, 2016.

ZIMBILI, O.; SALIM, W.; NDAMBUKI, M. A Review on the Usage of Ceramic Wastes in Concrete Production. **International Journal of Civil, Environmental, Structural, Construction and Architectural Engineering**, v. 8, n. 1, p. 91–95, 2014.

ACKNOWLEDGEMENTS

I want to thank Prof[a]. Dr[a]. Tatiana Pineda Vasques for the advices, support and patience throughout this study and UFSC for the access to digital libraries and structure through my graduate education. I am thankful and fortunate enough to get constant encouragement, support and guidance from all the teaching staff which helped me in successfully complete this journey. A special acknowledgement to Prof[a]. Dr[a]. Regina Vasconcellos for letting us use her laboratories, with all the equipment and materials needed.

I am deeply thankful for the support received from my family that always were there for me under any circumstances. I want to thank my friends from primary school for being friends with me until today and for always being there for me whenever I needed. Special regards to the friends I made during my graduation that helped in any way so this could happen. To all my roommates Lara and Jaqueline that made everything easier with their friendship and support. And I could not finish this without mentioning my boyfriend Paulo Jeremias for all the support and help and was there for me from the very start until the end. This accomplishment would not have been possible without them.